3.6 Bunch Compressor

3.6.1 Introduction

A detailed design for a single stage beam bunch length compressor for the TESLA Linear Collider is presented. Compression is achieved by introducing an energy-position correlation along the bunch with an RF section at zero-crossing phase followed by a short bending section with energy dependent path length (momentum compaction). The motivation for a wiggler design is presented and many of the critical single bunch tolerances are evaluated. A solenoid based spin rotator is included in the design and transverse emittance tuning elements, diagnostics and tuning methods are described. Bunch length limitations due to second order momentum compaction and sinusoidal RF shape are discussed with options for compensation.

3.6.2 Bunch Compressor Design Issues

The bunch compressor design is influenced by several criteria:

- The compressor must reduce the bunch length extracted fom the damping ring to the appropriate size in the linac.
- The system must perform a 90 degree longitudinal phase space rotation so that damping ring extracted phase errors do not translate into linac phase errors which can produce large final beam energy deviations.
- The system must not significantly dilute the transverse emittances and should include tuning elements for correction.
- With its low energy and initially small energy spread, the bunch compressor is a convenient place to include solenoids for full control of the spin orientation.
- The compressor should be short, simple and as error tolerant as possible.

3.6.3 Bunch Compressor Parameters

The rms bunch length at the entrance to the linac (for uncorrelated Damping Ring energy spread σ_{δ_0}) is

$$\sigma_{zl} = \sqrt{(1+\alpha k)^2 \sigma_{z_0}^2 + \alpha^2 \sigma_{\delta_0}^2} \tag{3.6.1}$$

with $\alpha \equiv \int \frac{\eta(s)}{\rho(s)} ds$ and $k = \frac{2\pi e V_0}{\lambda E_0}$, where η and ρ are dispersion and bending radius along the beam line while V_0 and λ are amplitude and wavelength of the RF system. E_0 is the beam energy.

The minimum bunch length is achieved when $\alpha = -1/k$ which also decouples the linac phase from the DR phase. The momentum compaction is chosen to achieve the desired linac bunch length and the rf voltage is then given:

$$\alpha = -\frac{1}{k} = \frac{\sigma_{z_l}}{\sigma_{\delta_0}} \qquad eV_0 = -\frac{\lambda_{rf} E_0}{2\pi\alpha}. \tag{3.6.2}$$

parameter	symbol	unit	
Energy	E_0	GeV	3.2
rms horizontal emittance	ϵ_x	mm-mrad	8.0
rms vertical emittance	ϵ_x	mm-mrad	0.13
rms DR bunch length	σ_{z_0}	mm	9
rms DR energy spread	σ_{δ_0}	%	0.1
rms linac bunch length	σ_{z_l}	mm	0.6
rms linac energy spread	σ_{δ_l}	%	1.4
rf wavelength	λ_{rf}	m	0.231
rf voltage	V_0	MV	190
rf gradient	G_{rf}	MV/m	25
length of rf section	L_{rf}	m	7.6
momentum compaction	α	m	0.64

Table 3.6.1: *Bunch compressor parameters. Emittance values represent those immediately after DR extraction and are smaller than the design values at the IP in order to have a safety margin.*

The resulting energy spread at the linac entrance is approximately amplified by the inverse of the bunch compression factor.

$$\sigma_{\delta_l} = \sigma_{\delta_0}\sqrt{\frac{\sigma_{z_0}}{\sigma_{z_l}} + 1} \approx \sigma_{\delta_0}\frac{\sigma_{z_0}}{\sigma_{z_l}} \quad , \quad (\sigma_{z_l} \ll \sigma_{z_0}) \tag{3.6.3}$$

The damping ring (DR) and initial linac parameters relevant for bunch compressor design are listed in Table 3.6.1.

3.6.4 Bunch Compressor Optics

A simple way to produce the necessary momentum compaction is with a chicane made of four horizontal bending magnets. A chicane of total length 24 m for the TESLA design is possible, however, the peak dispersion required is large at 1.8 m. With 1.5 % rms energy spread the horizontal beam size becomes very large (σ_x=27 mm) and dipole field quality tolerances become tight. A more error tolerant design is achievable with a wiggler section [1] made up of N_p periods each with two bending magnets and two quadrupoles-one at each zero crossing of the dispersion function. If the bends are rectangular and each of length L_B with angle θ_B and separated by ΔL, and the quadrupoles alternately reverse sign to produce a phase advance per cell of $\Psi_x(= \Psi_y)$, the momentum compaction, α_w, and the horizontal emittance growth due to synchrotron radiation (SR), $\Delta\gamma\epsilon_x$, are given by [1]:

$$\alpha_w = \frac{1}{4}\theta_B^2[N_p(2\Delta L + L_B) - \frac{1}{6}(2N_p + 1)L_B] \tag{3.6.4}$$

$$\Delta\gamma\epsilon_x \approx (1.25 \cdot 10^{-8} m^2 \cdot GeV^{-6}) \cdot E_0^6 N_p \frac{|\theta_B|^5(\Delta L + L_B)}{L_B^2 |sin\Psi_x|} \tag{3.6.5}$$

parameter	symbol	unit	
momentum compaction	α_w	meters	0.600
dipole magnet length	L_B	meters	2.0
bend-to-bend separation	D_L	meters	3.22
bend angle / dipole	ϕ_B	degrees	16.0
total length	L_{tot}	meters	47
maximum x-dispersion	η_{max}	mm	308
SR x-emittance dilution	$\Delta\epsilon_x/\epsilon_{x0}$	%	1.8
dipole magnetic field	B_0	kG	15.37
quad. pole tip fields - F (D)	B_Q	kG	2.0 (1.7)
number of periods	N_p	-	4
phase advance per period	q_x	degrees	90

Table 3.6.2: *Wiggler design parameters (NOTE: All non-correction quadrupoles in the entire beamline are of length 15 cm and pole-tip radius 1 cm).*

By setting the necessary momentum compaction [2] and choosing a horizontal SR emittance dilution of 1-2%, a dipole field strength of 15 kG, and roughly minimizing dipole magnet length and peak dispersion, the wiggler design parameters listed in Table 2 were developed. With $|\sin\Psi_x|^{-1}$ minimized at $\Psi_x = \pi/2$, the number of periods is chosen so that each dipole at peak dispersion has an opposing dipole separated by π in betatron phase advance: all orders of dispersion generated by equal multipole field components cancel. The peak horizontal beam size in the wiggler is 4.3 mm. The β and dispersion functions and a schematic beamline layout of the wiggler (including a 12 meter, 8 cavity TESLA superconducting rf module) are plotted in Fig. 3.6.2.

3.6.5 Peripheral Sections and the Full Beamline

In addition to the primary function of bunch compression, the beamline described here also includes sections for spin rotation, cross-plane coupling correction, and phase space diagnostics. This section describes these modules (for reference, the entire beamline is depicted in Fig. 3.6.2).

3.6.5.1 Spin Rotator

Using the TESLA damped vertical emittance, it can be shown [3] that for a chicane type "half serpent" $\pi/2$ spin rotator [4] constructed from horizontal and vertical bending magnets, and for $< 2\%$ SR vertical emittance dilution, the relationship between the length of the bending magnets and the beam energy is discouraging: $L[m] > 30 \cdot E[GeV]$. Even at 3.2 GeV the dipoles are about 100 m long. Therefore a spin rotator based on superconducting solenoids is proposed prior to bunch compression. Since the damped beam is flat ($\epsilon_y/\epsilon_x \ll 1$) the cross-plane coupling induced by the solenoids must be compensated. This is achieved by rotating the spin by $\pi/2$ around the longitudinal

parameter	symbol	unit	
momentum compaction	α_w	meters	0.600
effective solenoid length	L_{sol}	meters	2.275
maximum solenoid field	B_z	kG	38.0
total arc bend angle	ϕ	degrees	12.0
total length of rotator system	L_{tot}	meters	52
number of dipole magnets (12 degree arc)	N_{dipole}	-	4
dipole field	B_0	kG	6.1
SR x-emittance dilution	$\Delta\epsilon_x/\epsilon_{x0}$	%	$1 \cdot 10^{-3}$
momentum compaction of all arcs	α_a	m	0.02
chromatic ϵ_y dilution $(\sigma_{\delta 0}) = 0.1\%$)	$\Delta\epsilon_y/\epsilon_{y0}$	%	0.7
chromatic ϵ_y dilution $(\sigma_{\delta 0}) = 0.2\%$)	$\Delta\epsilon_y/\epsilon_{y0}$	%	4.6
chromatic ϵ_y dilution $(\sigma_{\delta 0}) = 0.3\%$)	$\Delta\epsilon_y/\epsilon_{y0}$	%	10.9

Table 3.6.3: *Spin rotator parameters*

axis with a pair of $\pi/4$ solenoids separated by a 'reflector' beamline which causes the solenoid pair's coupling to cancel while their spin precession adds. In this way the solenoid coupling is always canceled regardless of the solenoid settings as long as the solenoid pairs have equal strength ($\pm 2\%$). By separating two such solenoid pair systems with a $\pi/2$ spin rotation around the vertical axis (i.e. an arc of total bend angle $\theta = \pi/2\alpha\gamma$) full arbitrary control of the spin orientation is possible. The focusing effect of the solenoids is corrected with four matching quadrupoles per paired solenoid section. The matching quadrupoles are positioned between the paired solenoid sections and the central arc (see Fig. 3.6.2). At $\sim 0.1\%$ rms DR energy spread the emittance dilution due to chromatic coupling of the four solenoids together at maximum field is negligible at 0.7%. The parameters of the spin rotator system are given in Table 3.6.3.

3.6.5.2 Coupling Correction Section

In order to empirically correct anomalous cross-plane coupling due to either damping ring extraction errors or spin rotator errors, a skew correction section (SCS) is included immediately following the final rotator solenoid. The system is constructed from four small skew quadrupoles with zero nominal strength. The first and second skew quadrupoles are separated by betatron phases of $\Delta\Psi_x = \Delta\Psi_y = \pi/2$. This is also true for the third and fourth skew quadrupoles. The second and third are separated by $\Delta\Psi_x = \pi, \Delta\Psi_y = \pi/2$ such that the four skew quadrupoles orthogonally control the four coupling coefficients in the beam: $\langle x'y\rangle$, $\langle xy'\rangle$, $\langle xy\rangle$ and $\langle x'y'\rangle$, respectively. The four skew corrections are actually orthonormal in that the emittance sensitivity to each skew quadrupole is designed to be a constant (i.e. $\beta_x\beta_y$ is equal at each skew quadrupole). The relative emittance increase for one thin skew quadrupole of focal length f at beta functions of $\beta_x\beta_y$ is

$$\frac{\epsilon_y}{\epsilon_{y0}} = \sqrt{1 + \frac{\epsilon_{x0}}{\epsilon_{y0}}\frac{\beta_x\beta_y}{f^2}}. \tag{3.6.6}$$

With skew quadrupoles of 10 cm length, 1 kG pole tip fields and 1 cm radii, a factor of about two in emittance increase can be corrected per skew quadrupole.

3.6.5.3 Diagnostic Section

It is important to provide measurement capability after the bunch compressor so that the beam emittance and matching can be monitored and corrected before entrance into the main linac. Following the wiggler section is a simple set of three FODO cells with phase advance per cell of $\Delta\Psi_x = \Delta\Psi_y = \pi/4$. By placing four wire scanners [5] near the vertical focusing quadrupoles the ideal four-wire scanner phase sampling is available to make high precision emittance and beta function measurements in each plane. The nominal rms beam size at the scanners is chosen as 15 μm vertically and 80 μm horizontally. A matched beam is easily identified since in this case the beam sizes per plane are identical at each of the four wire scanners. The cross-plane coupling in the beam is not fully measurable with this section. However, by simply minimizing the vertical emittance (flat beam) with the four SCS skew quadrupoles all coupling can be corrected (with some iteration necessary in extreme cases). A direct measurement capability is achievable, if desired, by using six wire scanners with phase advances similar to the SCS described above [6].

3.6.5.4 Compressor RF Section

The energy-position correlation is introduced with one 12 meter superconducting TESLA accelerating module with eight cavities each of 1.035 meter length with gradient of 25.0 MV/m in order to produce the necessary 190 MV for full bunch compression.

3.6.5.5 The Combined Beamline

The four sections described thus far (spin rotator, coupling correction, bunch compressor and diagnostics) are combined using various appropriate matching quadrupoles to preserve the periodic beta functions in the various FODO cells. Fig. 3.6.2 shows the beta and dispersion functions of the combined system. The combined system floorplan is laid out in Fig. 3.6.1. The system, including the 3.1 meter spin rotator bump, should fit inside a 5 meter diameter tunnel. The angle of the first arc may be reduced and the angle of the third arc equally increased if it is necessary to horizontally displace the outgoing beamline relative to the incoming one. It is only necessary that the 12 degree arc remains fixed (for 3.2 GeV) so that the electron or positron spin orientation is fully controllable over a sphere.

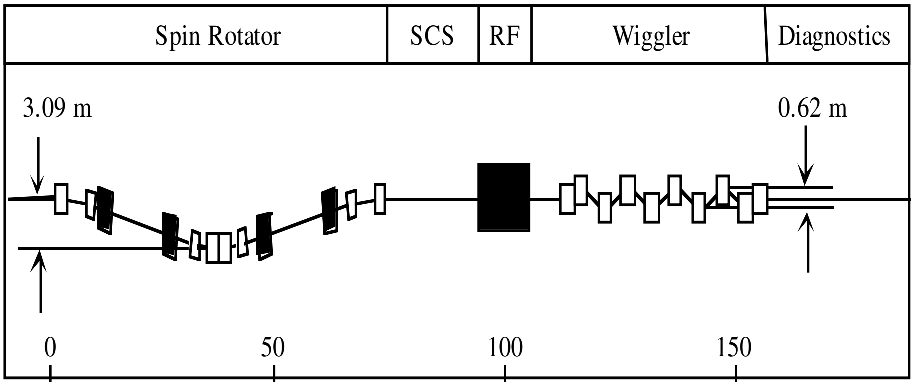

Figure 3.6.1: *Schematic layout of complete beamline floorplan. Solenoids and the RF-module are in black, dipole magnets are in white (quadrupole magnets not shown).*

3.6.6 Tolerances

3.6.6.1 Single Bunch Tolerances

The large energy spread and strong bending of the wiggler present some challenges for transverse emittance preservation, especially in the vertical plane. Several important tolerances are examined below. Table 4 evaluates these tolerances:

- A rolled dipole magnet introduces vertical dispersion which, if not corrected, will chromatically filament in the main linac and dilute the vertical emittance.
- A quadrupole (sextupole) field component in a dipole with horizontal dispersion will dilute the horizontal emittance through the generation of first (second) order horizontal dispersion. The symmetry of the wiggler optics introduces a strong cancellation of these two effects if the dipole field errors are similar for all magnets. This tolerance, when applied to the wiggler dipoles, can therefore be considered as a constraint on the field uniformity over the eight inner wiggler dipoles (the first and tenth have near zero dispersion).
- A misaligned quadrupole will generate vertical and/or horizontal dispersion.
- A rolled quadrupole in a non-dispersive section will couple the beams while a rolled quadrupole in a dominantly dispersive section will generate vertical dispersion. Table 4 lists a range of roll tolerances with the tightest tolerance on one of the matching quadrupoles just after the RF section and also on the quadrupole in the center of the 12 degree arc (see Fig. 3.6.2). The loosest tolerances are on the wiggler quadrupoles which are weak.
- There are also tolerances on the difference of the field strengths between the paired solenoids and also on the absolute gradient of the eight quadrupoles which make up the reflector beamline between the paired solenoids. These tolerances

tolerance	symbol	unit	
wiggler dipole magnet roll tolerance	$\lvert\phi\rvert$	μrad	80
quad. field in wiggler dipole (r0=20 mm)	$\lvert b1/b0\rvert$	-	$4.0 \cdot 10^{-5}$
sext. field in wiggler dipole (r0=20 mm)	$\lvert b2/b0\rvert$	-	$1.4 \cdot 10^{-4}$
F-quad. x-misalignment tolerance	$\lvert\Delta_x\rvert$	μm	460
D-quad. y-misalignment tolerance	$\lvert\Delta_y\rvert$	μm	70
Quadrupole roll tolerance range	$\lvert\phi\rvert$	mrad	3.5 - 14
Paired solenoid field difference tolerance	$\lvert\Delta b_z/B_{z-max}\rvert$	%	2
reflector quad. grad. tol. range (max. sol.)	$\lvert\Delta G/G_0\rvert$	%	0.4 - 1.7
compression RF phase stability tolerance	$\lvert\psi_{RF}\rvert$	degrees	0.33

Table 3.6.4: *Single element tolerances for TESLA wigglers and spin rotators for $< 2\%$ emittance dilution or $|\langle z_l\rangle| < \sigma_{z_l}/3$ longitudinal stability at the IP (no correction assumed).*

have been evaluated with tracking and are included in Table 3.6.4. These tolerances assume no correction. The reflector beamline quadrupole gradient tolerances are evaluated at the maximum solenoid field and vary over the eight quadrupoles. The tightest of the eight are for the two quadrupoles which are most centered between the paired solenoids.

- If the phase, ψ_{RF}, of the compression RF were to deviate from the zero crossing this energy offset will advance or delay the phase of the bunch as it enters the linac and upset the collision timing at the interaction point (IP).

The roll tolerances are quite tight and probably difficult to achieve. However, these tolerances can be relaxed by an order of magnitude by including small normal and skew quadrupoles of zero nominal field to be used for dispersion correction.

3.6.6.2 Damping Ring Extraction Phase Tolerances and Limits for Bunch Compression

The compression arguments presented thus far are limited to linear effects. In fact the bunch is not infinitely compressible and at some point second order momentum compaction limits the achievable bunch length. the second order momentum compaction, α_2, the linac bunch position of a particle has a quadratic dependence on its DR bunch position.

$$z_l = [\alpha + \alpha_2\delta_0]\delta_0 + (1 + k[\alpha + \alpha_2\delta_0])z_0 + \alpha_2 k^2 z_0^2 \approx \alpha\delta_0 + \alpha_2 k^2 z_0^2 \qquad (3.6.7)$$

The approximation made in eq. 3.6.7 is possible since $\alpha_2\delta_0 \ll \alpha$ and $k = -1/\alpha$. For a wiggler, the approximate relationship between the second and first order momentum compaction is

$$\alpha_2 \approx -\frac{3}{2}\alpha. \qquad (3.6.8)$$

For a DR bunch length distribution which is Gaussian (i.e. $\langle z_0^4 \rangle = 3\langle z_0^2 \rangle^2$) and 'full compression' ($k = -1/\alpha$), the linac rms bunch length is

$$\sigma_{z_l}^2 \approx \langle z_l^2 \rangle - \langle z_l \rangle^2 = \alpha^2 \sigma_{\delta_0}^2 + \frac{9}{2} \cdot \frac{\sigma_{z_0}^4}{\alpha^2} \tag{3.6.9}$$

If α is reduced in order to compress the bunch toward zero, the second term on the r.h.s. of eq. 3.6.9 begins to dominate the final bunch length. The minimum achievable bunch length is given by:

$$\sigma_{z_l-min} = \sqrt{3\sqrt{2}\sigma_{\delta_0}\sigma_{z_0}} \tag{3.6.10}$$

In addition to limiting the achievable bunch length, the second order momentum compaction also gives rise to a quadratic linac "phase" dependence on DR "phase". Thus, DR extraction "phase" errors, $\langle z_0 \rangle$, will transform into final beam energy deviations roughly depending on the mean accelerating RF phase in the main linac, $\langle \psi \rangle$ (=0 at RF crest). For small "phase" errors, $z_l \ll \lambda$, and including only the RF curvature in the main linac, final beam energy deviations, $\langle \delta_E \rangle$, can be approximated by

$$\langle \delta_E \rangle \approx -\frac{2\pi \tan\langle \psi \rangle}{\lambda} \cdot \langle z_l \rangle. \tag{3.6.11}$$

The DR extraction "phase" jitter tolerance is then:

$$|\langle z_0 \rangle| < \sqrt{\frac{|\langle \delta_E \rangle| \lambda \alpha}{3\pi |\tan\langle \psi \rangle|}}. \tag{3.6.12}$$

The necessary stability of the longitudinal beam position at the interaction point (IP) also sets a tolerance on DR "phase" jitter. The DR "phase" jitter tolerance for fraction bunch position IP stability of $|\langle z_l \rangle| < \sigma_{z_l}/n$ (e.g. n =3) is

$$|\langle z_0 \rangle|_{tol} < \sqrt{\frac{2\alpha\sigma_{z_l}}{3n}} \tag{3.6.13}$$

The bunch length is also limited by the sinusoidal character of the compressor RF. Including the 3rd order term of the $\sin(z_0)$ expansion and not including the second order momentum compaction, the bunch position of a particle in the linac, for full compression where $k = -1/\alpha$, is

$$z_l \approx \alpha\delta_0 + \frac{1}{6}\left(\frac{2\pi}{\lambda}\right)^2 \cdot z_0^3, \tag{3.6.14}$$

and for a DR bunch length distribution which is initially gaussian, the rms bunch length is

$$\sigma_{z_l}^2 \approx \alpha^2 \sigma_{\delta_0}^2 + \frac{5}{12} \cdot \left(\frac{2\pi}{\lambda}\right)^4 \cdot \sigma_{z_0}^6 \tag{3.6.15}$$

parameter	symbol	unit	
linac linear bunch length	σ_{zl}	mm	0.56
linac frequency	f_{RF}	GHz	1.3
linac mean acc. phase	$\langle\psi\rangle$	degrees	3.3
The following include the effect of second order momentum compaction only.			
linac rms 2nd order bunch length	σ_{zl}	mm	0.63
min. 2nd order linac bunch length	σ_{zl-min}	mm	0.56
DR "phase" tol. for $\langle\delta_E\rangle < 0.01\%$	$\lvert\langle z_0\rangle\rvert_{tol}$	mm (deg)	5 (8)
DR "phase" tol. for $\lvert z_l\rvert/\sigma_{z_l} < 1/3$	$\lvert\langle z_0\rangle\rvert_{tol}$	mm (deg)	9.2 (14)
The following include the effect of the sinusoidal RF only.			
linac rms sinusoidal bunch length	σ_{z_l}	mm	0.65
min. rms sinusoidal linac b.l.	σ_{z_l-min}	mm	0.34
DR "phase" tol. for $\langle\delta_E\rangle < 0.01\%$	$\lvert\langle z_0\rangle\rvert_{tol}$	mm (deg)	8 (12.5)
DR "phase" tol. for $\lvert z_l\rvert/\sigma_{z_l} < 1/3$	$\lvert\langle z_0\rangle\rvert_{tol}$	mm (deg)	12 (18)
The following includes both non-linear bunch length limitations.			
linac rms bunch length	σ_{z_l}	mm	0.70

Table 3.6.5: *Bunch length limits and DR phase jitter tolerances, due to second order momentum compaction and sinusoidal compressor RF each taken in isolation. The DR extracted bunch length distribution is taken as a Gaussian for these calculations. The phase tolerances specified in deg. are w.r.t. the compressor-RF. They are smaller by a factor of three for the damping ring RF-system.*

In this case the minimum achievable bunch length is in the direction $\alpha \to 0$. The DR extraction "phase" jitter tolerance due to the sinusoidal RF is given by

$$|\langle z_0\rangle|_{tol} < \frac{\lambda}{2\pi}\left(\frac{6|\delta_E|}{|\tan\langle\psi\rangle|}\right)^{\frac{1}{3}} \tag{3.6.16}$$

Required IP longitudinal stability sets a DR "phase" jitter tolerance of

$$|\langle z_0\rangle|_{tol} < \left(\frac{6\sigma_{z_l}}{n}[\frac{\lambda}{2\pi}]^2\right)^{\frac{1}{3}} \tag{3.6.17}$$

Bunch length limitations and DR phase jitter tolerances for both second order momentum compaction and sinusoidal RF effects are summarized below in Table V. It can be shown that the two non-linear bunch length limitations discussed above approximately add in quadrature. The net rms bunch length, including both effects, is listed at the end of the table. Note, with these non-linear effects the rms bunch length results are somewhat dependent on the initial DR extracted bunch distribution-taken as a Gaussian here.

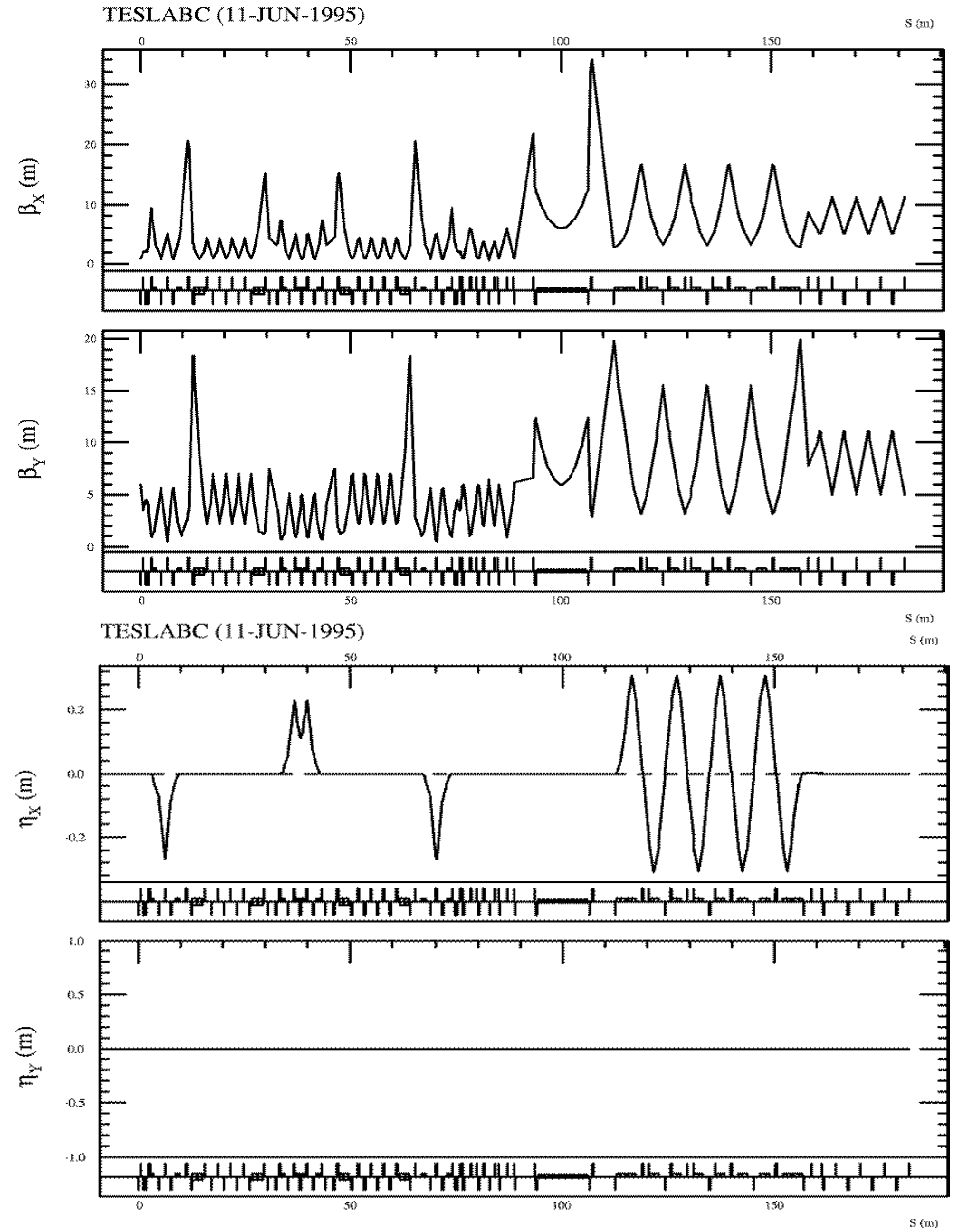

Figure 3.6.2: *β and dispersion functions for wiggler and RF section. Dipole magnets are shown as low rectangles biased above the beam line while the eight RF structures are centered. Horizontal focussing quadrupoles are biased above, vertical focusing quads below the beam line.*

Bibliography

[1] T. O. Raubenheimer, P. Emma, S. Kheifets, *Chicane and Wiggler Based Bunch Compressors for Future Linear Colliders*, Proc. of the 1993 Particle Accelerator Conference, Washington, D.C., 1993.

[2] The momentum compaction has been chosen slightly smaller than the linear design would require in order to somewhat compensate for RF non-linearities.

[3] P. Emma, *A Spin Rotator System for the NLC*, NLC-NOTE 7, December 1994.

[4] T. Fieguth, *Snakes, Serpents, Rotators and the Octahedral Group*, SLAC-PUB-4195, January, 1987.

[5] The term ”wire scanner” may refer to a laser wire rather than a metallic filament, depending on survivability details. However, it will be prudent to include simple, well tested metallic filament type wire scanners for single bunch measurement to initially commission the beamline.

[6] P. Emma, *A Skew Correction and Diagnostic Section for Linear Colliders*, NLC-NOTE in preparation.